



Double-detecting fluorescent sensor for ATP based on Cu²⁺ and Zn²⁺ response of hydrazono-bis-tetraphenylethylene

Shengjie Jiang^a, Jiabin Qiu^a, Shibing Chen^a, Hongyu Guo^a, Fafu Yang^{a, b, c, *}

^a College of Chemistry and Materials, Fujian Normal University, Fuzhou, 350007, PR China

^b Fujian Key Laboratory of Polymer Materials, Fuzhou, 350007, PR China

^c Fujian Provincial Key Laboratory of Advanced Materials Oriented Chemical Engineering, Fuzhou, PR China

ARTICLE INFO

Article history:

Received 4 July 2019

Received in revised form

12 September 2019

Accepted 24 September 2019

Available online 17 October 2019

Keywords:

Tetraphenylethylene

Fluorescent sensor

Double detect

ATP

Zn²⁺

Cu²⁺

ABSTRACT

Although all kinds of sensors with unique detecting ability for one guest were reported, the fluorescence sensor with multiple detecting abilities was seldom presented. This work designed and synthesized a novel AIE fluorescence probe bearing double detecting for ATP based on Cu²⁺ and Zn²⁺ response of hydrazono-bis-tetraphenylethylene (**Bis-TPE**). **Bis-TPE** was prepared in 82% yield with simple procedure. It exhibited strong red AIE fluorescence based on the large conjugated electron effect in aqueous media. It showed outstanding selective sensing abilities for Cu²⁺ by strong fluorescence quenching and for Zn²⁺ by red-orange fluorescence change. The sensing mechanism of 1:1 stoichiometric ratios was confirmed by ¹H NMR and MS study. The strong red fluorescence of **Bis-TPE** + Cu²⁺ system could be recovered by adding ATP. The orange fluorescence of **Bis-TPE** + Zn²⁺ system could be quenched by adding Cu²⁺ and then was recovered by adding ATP. These double detecting abilities for ATP with the “off-on” red fluorescence in **Bis-TPE** + Cu²⁺ system and “allochroic-off-on” orange fluorescence in **Bis-TPE** + Zn²⁺+Cu²⁺ system were successfully applied to test Cu²⁺, Zn²⁺ and ATP in test paper and living cell imaging, displaying the good application prospects for sensing Cu²⁺, Zn²⁺ and double detecting ATP in the complicated environment.

© 2019 Elsevier B.V. All rights reserved.

1. Introduction

In the past decades, the fluorescent sensors were paid much attention in detecting ions and biomolecules due to their obvious advantages of high sensitivity, low cost, and simple operation [1–6], avoiding the restriction of huge equipment, long times, high cost, complicated and professional operation of the other detection methods such as atomic absorption spectroscopy (AAS), atomic fluorescence spectrometry (AFS) and inductively coupled plasma mass spectrometry (ICP-MS) [7,8]. Many traditional dyes, such as BODIPY, fluorescein, rhodamine and cyanine were modified as excellent fluorescent probes for sensing anionic ions, cationic ions, biological molecules, etc. [9–14]. However, although these fluorescent probes usually possessed high fluorescence in organic solvents, the strong aggregation-caused quenching (ACQ) effect in aqueous solution seriously limited their practical application. In 2001, Tang's group reported the aggregation induced emission

(AIE) phenomenon, which eliminates effectively the ACQ effect [15]. From then on, AIE molecules had been studied extensively and exhibited the widely application in numerous fields, such as luminous liquid crystal [16–19], organic light-emitting diodes (OLED) [20–22], circularly polarized photoluminescence [23,24], as well as ion detection and biomolecular recognition in aqueous media [25–33].

It was well known that the contamination of heavy metals is a kind of serious threat to human health and causes series of diseases usually [34,35]. For instance, copper leads to Menkes syndrome [36]. Cobalt induces radiation skin damages, and mercury disturbs the central neural system [37,38]. The abnormal zinc levels might result in immune dysfunction diseases such as brain diseases, diabetes, epilepsy, Alzheimer's and Parkinson's disease [39–42]. On the other hand, phosphates play important roles in biological systems [43]. Among various phosphate anions, adenosine triphosphate (ATP) is one of the most important species due to its pivotal functions for both intracellular energy supplier and extracellular signalling mediator in metabolic processes [44,45]. Up to now, all kinds of fluorescence sensors including AIE sensors had been applied for detecting heavy metallic ions, ATP and other guests, respectively [46–55]. Generally, the AIE sensor displayed the

* Corresponding author. College of Chemistry and Materials, Fujian Normal University, Fuzhou, 350007, PR China.

E-mail address: yangfafu@fjnu.edu.cn (F. Yang).

detecting ability for one kind of metallic ion, one kind of metallic ion and/or ATP, or two kinds of metallic ions such as for Hg^{2+} and Ag^+ , Zn^{2+} and Cd^{2+} , or Fe^{3+} and Hg^{2+} [56–58]. Obviously, by comparison with the sensor for detecting only one kind of metallic ion and/or ATP, the sensor for selectively detecting multiple metallic ions and/or ATP has the advantage of higher efficiency, cheaper cost and more simplified operation for practical application. However, such fluorescence sensor bearing multiple detecting abilities was seldom prepared so far. In this paper, we wish to report a novel AIE hydrazono-bridged bis-tetraphenylethylene sensor, which possessed the good sensing abilities for Zn^{2+} , Cu^{2+} and ATP with double detecting processes based on the responses of “off-on” red fluorescence and “allochroic-off-on” orange fluorescence, respectively. Moreover, it was successfully applied in test paper and living cell bioimaging, exhibiting the good application prospects in sensing Cu^{2+} , Zn^{2+} and double detecting ATP in complicated environment and living body.

2. Experimental section

2.1. Materials and methods

All chemical reagents were obtained from Aladdin Reagent Co., Ltd. and were used directly. The pre-coated glass plates were used for TLC analysis. Silica gel (100–200 mesh) was applied for column chromatography. NMR spectra were recorded on a Bruker-ARX 400 instrument at 25 °C. MS spectra were measured on Bruker mass spectrometer. PerkinElmer 2400 CHN Elemental Analyzer was used for elemental analyses. Fluorescent spectra were examined on a Hitachi F-4500 spectrometer with conventional quartz cell (10 × 10 × 45 mm) at 25 °C. The fluorescence absolute quantum yield (Φ_F) was obtained on an Edinburgh Instruments FLS920 Fluorescence Spectrometer with a 6-inch integrating sphere. Compound **3** was synthesized by reacting 2-hydroxybenzophenone and benzophenone in Zn, TiCl_4 /THF system according to the published literature [59].

2.2. Synthetic procedure for compound 4

The mixture of compound **3** (0.35 g, 1 mmol) and methenamine (0.84 g, 6 mmol) were stirred and refluxed in 10 mL of HOAc overnight. TLC detection suggested the disappearance of starting material. After reaction, 50 mL of 1 M HCl solution was poured into the reaction mixture, and then extracted with CHCl_3 (20 mL × 3). The organic phase was collected and concentrated under reduced pressure. The residue was purified by column chromatography (eluent: CH_2Cl_2 /hexane = 1/2) to afford compound **4** as pale yellow solid in yield of 54%. ^1H NMR (400 MHz, CDCl_3): δ ppm: 10.92 (s, 1H, OH), 9.58 (s, 1H, CHO), 7.02–7.19 (m, 17H, ArH), 6.72 (d, J = 8.0 Hz, 1H, ArH). MALDI-TOF-MS ($\text{C}_{27}\text{H}_{20}\text{O}_2$) Calcd. for m/z = 376.146, found: m/z = 376.432 (M^+).

2.3. Synthesis procedure of Bis-TPE

Compound **4** (0.376 g, 1 mmol) and 0.025 mL of hydrazine hydrate were added to 20 mL of absolute ethanol. The mixture was refluxed and stirred for 12 h under the TLC detection. After the reaction, the solvents were removed by reduced pressure and the residue was recrystallized from CHCl_3 /MeOH to afford Bis-TPE as yellow powder (82% yield). ^1H NMR (400 MHz, CDCl_3) δ ppm: 11.25 (s, 1H, OH), 8.36 (s, 1H, N=CH), 7.00–7.26 (m, 16H, ArH), 6.97 (s, 1H, ArH), 6.74 (d, J = 8.0 Hz, 1H, ArH). ^{13}C NMR (100 MHz, CDCl_3) δ ppm: 164.52, 158.36, 143.60, 143.36, 140.90, 139.33, 136.65, 135.32, 131.36, 131.27, 127.95, 127.81, 127.58, 126.66, 126.46, 116.70, 117.47. MALDI-TOF-MS ($\text{C}_{54}\text{H}_{40}\text{N}_2\text{O}_2$) Calcd. for m/z = 748.309, found: m/z = 748.379 (M^+). Anal. calcd for $\text{C}_{54}\text{H}_{40}\text{N}_2\text{O}_2$: C 86.60, H 5.38, N

3.74; found C 86.66, H 5.33, N 3.69.

2.4. The tested procedure of the test paper

Pieces of filter paper were immersed in THF- H_2O (5:95) solution of Bis-TPE (0.1 mM) for 2 min. Then the filter papers were volatilized in air at room temperature. After that, the filter papers were customized as round slices. Three drops of a solution containing 0.1 mM of different metal ions (none, Ag^+ , Cd^{2+} , Cr^{3+} , Fe^{3+} , Hg^{2+} , K^+ , Na^+ , Pb^{2+} , Cu^{2+} , Sr^{2+} , Mg^{2+} , Zn^{2+} , Al^{3+} , Co^{2+} , Ni^{2+} and Ca^{2+}) or ATP were added to the test paper. After drying, the slices were observed under UV-light (365 nm).

2.5. MTT assay

Methylthiazolyldiphenyl-tetrazolium (MTT) trials were done to determine the toxicity for MCF-7 cancer cells. The inoculated MCF-7 cancer cells were cultivated at 37 °C and 5% CO_2 for 24 h, then 1.0×10^{-5} M of Bis-TPE was tracked in the cells after incubating for 24 h. The fostered cells were rinsed by PBS buffer, and continue cultivating for 3 h, in 0.5 mg/mL MTT-PBS buffer. Further, 100 μL of DMSO was added into dissolve the generated Formazan crystals, and detected the absorption intensity at 490 nm.

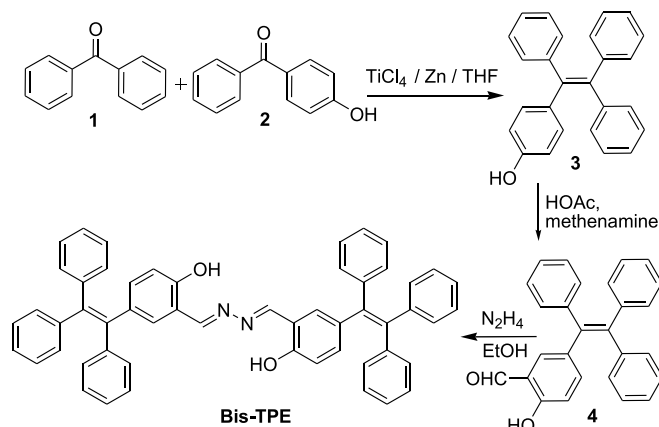
2.6. The experiment of living cell imaging. Bis-TPE

(3.0 mg) was dissolved in 1 mL of DMSO and then diluted with PBS buffer (pH = 7.4) to concentration of 1.0×10^{-5} M for imaging test. MCF-7 cancer cells were cultivated under the above identical circumstance of MTT trials for 24 h, and then being tinted by 1.0×10^{-5} M of Bis-TPE with 24 h breeding. After rinsing with PBS-buffer, dyed cells were cultivated in solution of metallic ions (1.0×10^{-5} M) or M^{2+} +ATP solution (1.0×10^{-5} M) for 1 h at 37 °C, respectively. The cells were imaged by a confocal laser scanning microscope (CLSM, Zeiss LSM 710, Jena, Germany).

3. Results and discussion

3.1. Synthesis and characterization

The synthetic route was shown as Scheme 1. According to the reported procedure [59], mono-hydroxy tetraphenylethylene **3** was synthesized by reacting benzophenone and mono-hydroxybenzophenone in Zn, TiCl_4 /THF system in yield of 32%. Then, by the classical formylation process under the reaction condition of HOAc/methenamine, compound **3** was converted to compound **4** in yield of 54%. Furthermore, the target hydrazono-bridged Bis-TPE



Scheme 1. The synthetic route for target Bis-TPE.

was prepared by refluxing compound **4** with hydrazine hydrate in yield of 82% after recrystallization. The structure of the **Bis-TPE** was characterized by ^1H and ^{13}C NMR spectroscopy, MALDI-TOF mass spectrometry and elemental analysis (see SI). All the characterization data supported its structure. For example, two singlets for $\text{N}=\text{CH}$ and OH appeared at 11.25 and 8.36 ppm, respectively, which suggested the symmetric *trans*-structure for $\text{C}=\text{N}$ groups of **Bis-TPE** as shown in Scheme 1.

3.2. AIE property

Tetraphenylethylene (TPE) is a typical AIE group. Thus, the AIE property of **Bis-TPE** was firstly investigated in the THF- H_2O mixture solution. The changes of fluorescence spectra and intensities of **Bis-TPE** with $\lambda_{\text{ex}} = 360$ nm in a series of THF- H_2O solutions were exhibited in Fig. 1 and Fig. S5. It can be seen that the changes of fluorescence intensities from $f_w = 0\%$ to 50% were negligible. But the emission intensities increased rapidly when $f_w > 60\%$, reaching its maximum value at $f_w = 95\%$. By comparison with that in pure THF solution, the fluorescence intensity of **Bis-TPE** increased by 6.4 times in THF- H_2O solution with 95% water content. The fluorescence quantum yield was 0.56 in THF- H_2O solution with 95% of H_2O . The fluorescence spectrum of **Bis-TPE** at solid state was also investigated as shown in Fig. S6. It displayed the strong solid fluorescence with fluorescence quantum yield of 0.63. All these results suggested the excellent AIE fluorescence for **Bis-TPE** at aggregated state. On the other hand, the fluorescence wavelength appeared at 550-700 nm with red color, which exhibited huge red shift than that of normal TPE derivatives (450-550 nm usually). This phenomenon could be attributed to the favorable influence of the conjugated electron effect of the structure of hydrazono-bridged **Bis-TPE**. This characteristic is an obvious advantage for the probe in living body, because the long wavelength emission benefits for the deep tissue permeation, minimum self-absorption and low background noise, etc. Moreover, **Bis-TPE** in THF- H_2O with $f_w = 95\%$ had good fluorescence stability in 24 h under normal daylight lamp (Fig. S7). As the highest fluorescence appeared in THF- H_2O with $f_w = 95\%$, this solution system was chosen for the further investigation on sensing guests.

3.3. The sensing abilities for metal ions

As a useful probe, it is essential to achieve a selective and sensitive response to the target analytes. Therefore, the selective response of **Bis-TPE** to different metal ions was investigated by UV-vis spectra and fluorescence spectra. Figs. S8 and S9 displayed the

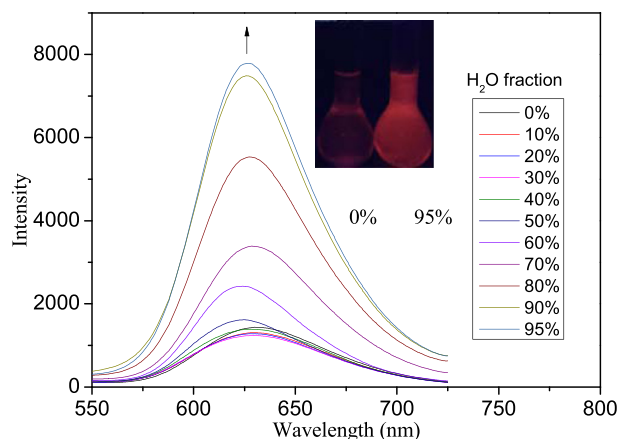


Fig. 1. The emission spectra of **Bis-TPE** in THF/ H_2O solutions with different fractions of H_2O ($1 \mu\text{M}$, $\lambda_{\text{ex}} = 360$ nm).

UV-vis spectra of **Bis-TPE** with various ions and Zn^{2+} at different concentrations. Although these UV-vis spectra exhibited some fluctuation at maximum absorption, no change for maximum absorption wavelength and no selectivity for ion were observed obviously. As to the fluorescence behaviours of **Bis-TPE** (Fig. 2), the fluorescence spectra with different metal ions (Ag^+ , Cd^{2+} , Cr^{3+} , Fe^{3+} , Hg^{2+} , K^+ , Na^+ , Pb^{2+} , Sr^{2+} , Mg^{2+} , Al^{3+} , Co^{2+} , Ni^{2+} and Ca^{2+}) fluctuated obviously. The maximum deviation percentages of fluorescence intensities were -8.6% for Hg^{2+} and $+29\%$ for Co^{2+} . On the other hand, the fluorescence spectra of **Bis-TPE** with Cu^{2+} and Zn^{2+} exhibited dramatically changes. The fluorescence was completely quenched by the addition of Cu^{2+} . When Zn^{2+} was added, the fluorescence enhanced remarkably and exhibited obvious blue shift (from 626 nm to 602 nm), accompanying by the color change from red to orange under ultraviolet lamp (as shown in Fig. 2). These results suggested that **Bis-TPE** possessed the good sensing ability for Cu^{2+} and Zn^{2+} simultaneously with the obvious phenomena of fluorescence quenching and color change, respectively.

3.4. Fluorescence titration for Cu^{2+} and Zn^{2+}

In order to further investigate the sensing properties of **Bis-TPE** for Cu^{2+} and Zn^{2+} , the fluorescence titration experiments were performed by varying the concentrations of Cu^{2+} and Zn^{2+} ions (0–3.0 equiv) in THF- H_2O (5:95) mixtures. As shown in Fig. 3a, with the increase of the concentration of Cu^{2+} , the intensities of the emission of **Bis-TPE** gradually decreased and the fluorescence was almost quenched completely when 2.0 equiv Cu^{2+} added. In Fig. 3b, with the increasing of concentrations of Zn^{2+} , the fluorescence intensities increased gradually and the maximum fluorescence wavelength exhibited blue shift. Based on these changes of fluorescence spectra, the corresponding plot of fluorescence intensities versus concentrations of metal ions was presented in Fig. S10. Both Fig. S10a and S10b displayed a good linear relationship for the systems with 0.0 to 1.0 equivalent concentrations of metal ions (as shown in inset part). According to the calculation formula $\text{DL} = K \times \text{Sb1}/S$ (where $K = 2$ or 3 , in this case the value = 2, Sb1 is the standard deviation of the blank solution, S is the value of the slope of the regression line), the detection limits can be calculated as $\text{DL} = 2.51 \times 10^{-7} \text{ M}$ for Cu^{2+} and $4.85 \times 10^{-7} \text{ M}$ for Zn^{2+} , respectively. The linear relationships also indicated the 1:1 binding stoichiometric ratios for **Bis-TPE** with Cu^{2+} and Zn^{2+} , which were further confirmed by the Job's plots as shown in Figure S11. It can be

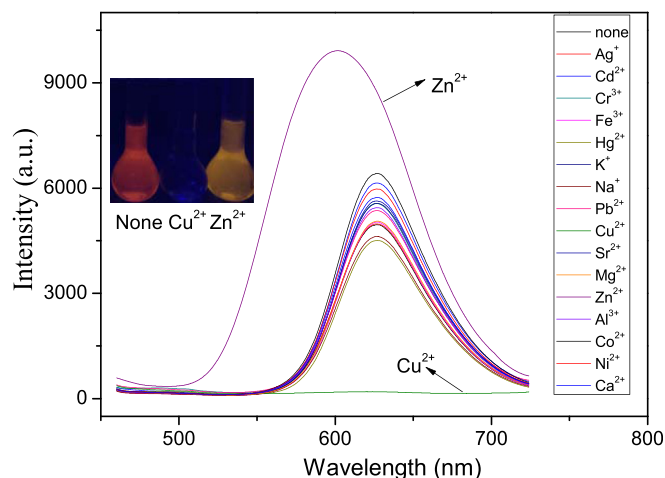


Fig. 2. Fluorescence spectra of **Bis-TPE** ($1 \mu\text{M}$) with different metal ions ($3 \mu\text{M}$) in THF- H_2O solution (5:95, V/V). $\lambda_{\text{ex}} = 360$ nm.

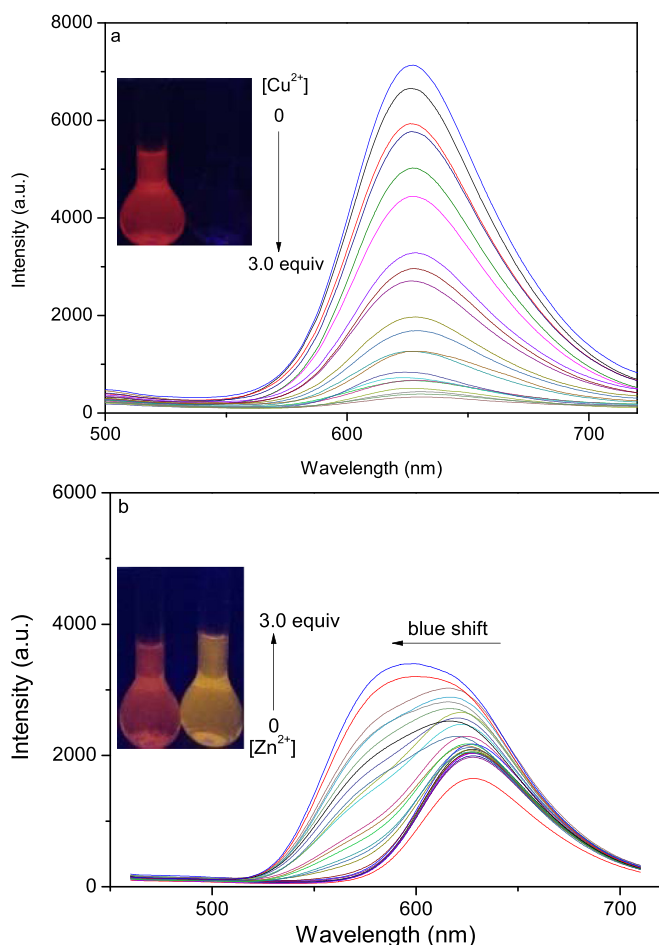


Fig. 3. Fluorescence spectra of **Bis-TPE** (1 μM) upon gradual addition of increasing amounts of (a) Cu^{2+} (0–3.0 equiv), (b) Zn^{2+} (0–3.0 equiv). Inset: Fluorescence images of **Bis-TPE** without and with Cu^{2+} and Zn^{2+} (1 μM), respectively.

seen that the break points for the change of fluorescence intensities were 0.5, implying strongly the 1:1 binding stoichiometric ratios of **Bis-TPE** for Cu^{2+} and Zn^{2+} .

3.5. Interference experiments

The sensing selectivity of **Bis-TPE** for Cu^{2+} and Zn^{2+} were further studied by competition experiments with other metal ions. The results were shown in Figure S12. It can be seen that the values of I/I_0 (indicating the changes of maximum fluorescence intensities of **Bis-TPE** with Cu^{2+} before and after adding interfering metal ions) were close to 1 (0.95–1.05, Figure 12a), suggesting the little influence of the competing metal ions on the sensing abilities of **Bis-TPE** for Cu^{2+} . These values suggested that the fluorescence of **Bis-TPE** with Cu^{2+} were almost not interfered by other ions. On the other hand, as to Zn^{2+} , the values of I/I_0 were near 1 in presence of all kinds of metallic ions except Cu^{2+} ($I/I_0 = 0.068$ for Cu^{2+} , Figure 12b), implying that the fluorescence of **Bis-TPE** with Zn^{2+} was quenched by adding Cu^{2+} . This phenomenon might indicate that the complexation ability of **Bis-TPE** for Cu^{2+} was stronger than that for Zn^{2+} , resulting in the substitution of Zn^{2+} by Cu^{2+} after adding Cu^{2+} in **Bis-TPE** + Zn^{2+} solution.

3.6. pH influence on sensing stabilities for Cu^{2+} and Zn^{2+}

The sensing stabilities under different pH are important for evaluating sensor performance in practical application. Thus, the

sensing stabilities of **Bis-TPE** for Cu^{2+} and Zn^{2+} were investigated at different pH conditions. As shown in Fig. S13, **Bis-TPE** has good fluorescence stability over a wide pH range of 4–10. As to **Bis-TPE** with Cu^{2+} , its fluorescence quenched remarkably and the good fluorescence stabilities were observed between pH = 4–10. The fluorescence intensities of **Bis-TPE** with Zn^{2+} increased obviously and exhibited wider stable ranges at pH = 2–11. These data indicated that **Bis-TPE** had good sensing stabilities for Cu^{2+} and Zn^{2+} in wide ranges of pH values, which were favorable for the practical application on analyzing samples.

3.7. The crystal data and sensing mechanism

A single crystal of **Bis-TPE** for X-ray diffraction analysis was obtained by slowly evaporating in dichloromethane. As shown in Fig. 4, tetraphenylethylene units adopted a highly distorted conformation. The dihedral angles between the four phenyl moieties of the TPE unit and the C=C double bond were 56.68°, 57.91°, 55.94° and 59.24°, respectively. The two phenyl moieties bridged by hydrazono group were coplanar and the *trans*-structure was observed for C=N bonds.

The ¹H NMR spectra of **Bis-TPE** with Cu^{2+} and Zn^{2+} were investigated as shown in Fig. 5. The protons of both OH and N=CH displayed obvious shifts and no split appeared, suggesting that the two OH groups and C=N groups were involved the sensing metal ions equally. Fig. S14 illustrated the MS spectra of **Bis-TPE** with excess Cu^{2+} and Zn^{2+} , in which the 1:1 stoichiometric peaks at 811.266 for Cu^{2+} and 813.393 for Zn^{2+} were observed and no other stoichiometric peak was detected. These 1:1 stoichiometric ratios were in accordance with the previous fluorescence Job's plots in Fig. S11. The fluorescence changes of **Bis-TPE** + Cu^{2+} (1:1, 1 μM) at 25, 30, 35, 40 °C were investigated and the results were shown in Figure S15. The fluorescence increased gradually with the increase of the temperature. These phenomena also supported the formation of **Bis-TPE** + Cu^{2+} complex since the higher temperature resulted in the dissociation of weakly bound complexes. Thus, based on the analyses of ¹H NMR spectra and MS spectra, the sensing mechanism of **Bis-TPE** for Cu^{2+} and Zn^{2+} was proposed as Figure S16. The similar spectra changes for ligands with Cu^{2+} and Zn^{2+} was also observed in other fluorescence sensor system [60,61]. The fluorescence quenching after adding Cu^{2+} could be ascribed to the chelation-enhanced quenching (CHEQ) derived from the ligand-to-metal charge transfer (LMCT) based on its strong paramagnetic property. The fluorescence enhancement after adding Zn^{2+} can be attributed to the chelation-enhanced fluorescence (CHEF) effect, which suppressed effectively the photoinduced electron transfer (PET) process.

3.8. Off-on and allochroic-off-on responses for double detecting of ATP

It had been confirmed that ATP has excellent binding abilities of

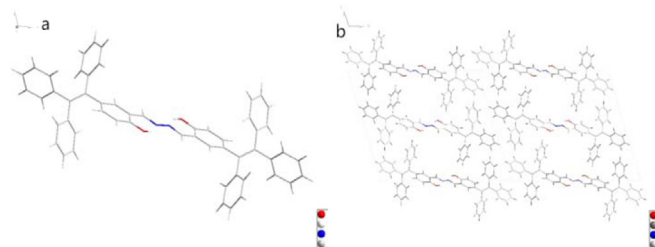


Fig. 4. (a) The ORTEP crystal diagram of a **Bis-TPE**, (b) The unit cell of **Bis-TPE** (see CCDC 1910867).

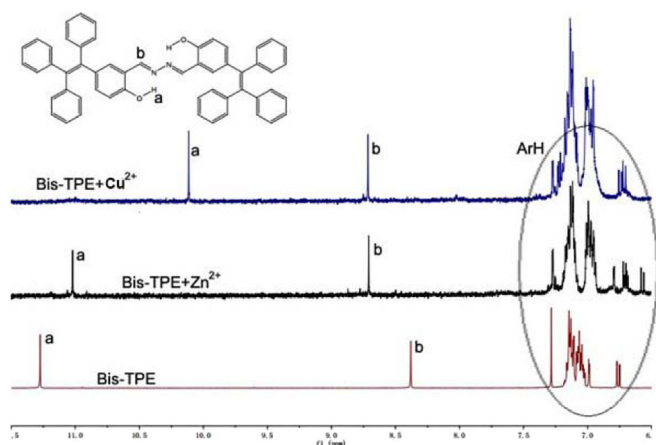


Fig. 5. ^1H NMR spectral changes of **Bis-TPE** upon the addition of 1.0 equiv of Cu^{2+} and Zn^{2+} , respectively.

Cu^{2+} based on the multiple complexed sites [53]. Thus, the sensing systems of **Bis-TPE** for Cu^{2+} and Zn^{2+} were applied for further sensing ATP. In a typical experiment, the solution of **Bis-TPE** (1 μM)

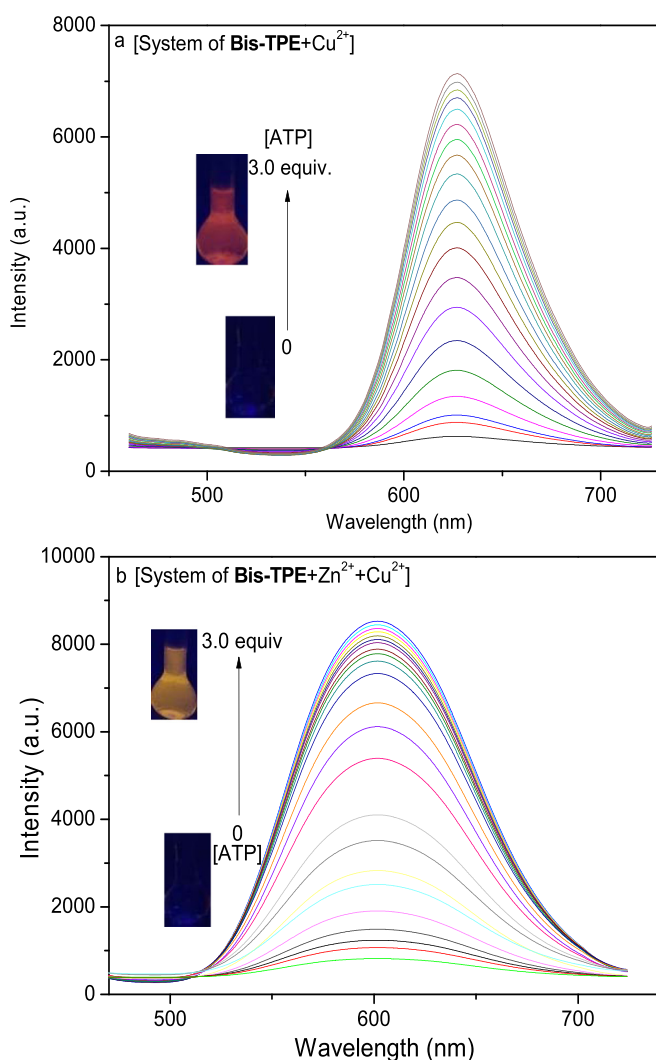


Fig. 6. (a) Fluorescence spectra of **Bis-TPE** (1 μM) with Cu^{2+} (2 μM) upon gradual addition of increasing amounts of ATP (0–3.0 equiv), (b) Fluorescence spectra of **Bis-TPE** (1 μM) with Zn^{2+} (2 μM) and Cu^{2+} (2 μM) upon gradual addition of increasing amounts of ATP (0–3.0 equiv).

with Cu^{2+} (2 μM) or **Bis-TPE** (1 μM) with Zn^{2+} (2 μM) and Cu^{2+} (2 μM) were prepared beforehand. Then ATP (0–3.0 equiv) was added and the fluorescence changes were measured as shown in Fig. 6. It could be seen that the quenched fluorescence in these two systems were recovered gradually. The red fluorescence for system of **Bis-TPE** with Cu^{2+} (Fig. 6a) and the orange fluorescence for system of **Bis-TPE** with Zn^{2+} and Cu^{2+} (Fig. 6b) were turned on obviously with the increase of ATP. Moreover, based on Fig. 6, the corresponding plot of fluorescence intensities versus concentrations of ATP were displayed in Figure S17. Both Figure S17a and S17b exhibited a good linear relationship for the systems with 0.0 to 2.0 equivalent concentrations of ATP. According to the calculation formula $\text{DL} = K \times \text{Sb1}/S$ (where $K = 2$ or 3 , the value = 2 in this case, Sb1 is the standard deviation of the blank solution, S is the value of the slope of the regression line), the detection limits of ATP could be counted as $\text{DL} = 4.23 \times 10^{-7} \text{ M}$ for system of **Bis-TPE** with Cu^{2+} and $1.04 \times 10^{-7} \text{ M}$ for system of **Bis-TPE** with Zn^{2+} and Cu^{2+} , respectively, revealing the good application prospect for the quantitative detection of ATP.

Based on the above fluorescence recovery of system of **Bis-TPE** with Cu^{2+} and **Bis-TPE** with Zn^{2+} and Cu^{2+} , the multiple detecting

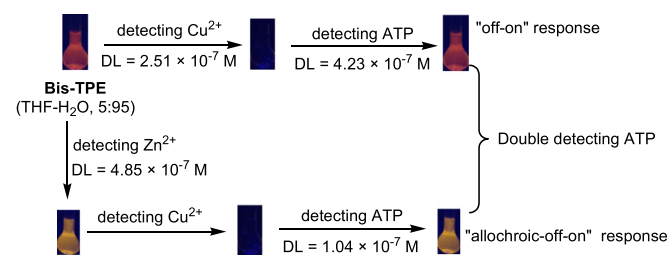


Fig. 7. The processes of double response for detecting ATP.

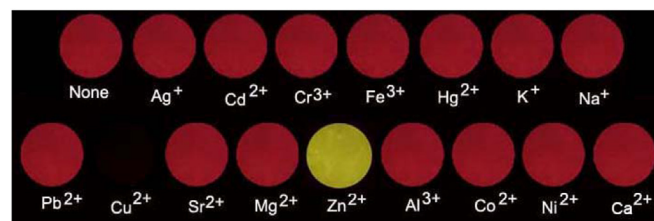


Fig. 8. Photographs of test slices with different ions under UV light (365 nm).

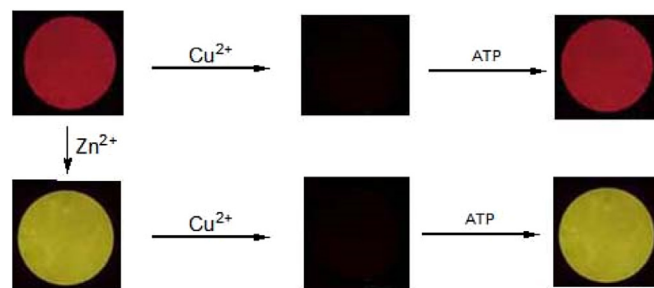


Fig. 9. Photographs of test slices of **Bis-TPE** for double detecting ATP with off-on and allochroic-off-on response under UV light (365 nm).

Table 1
Determination of Cu^{2+} and Zn^{2+} in real samples using **Bis-TPE** and ICP-MS.

Sample	Using Bis-TPE	Using ICP-MS
Cu^{2+}	91 $\mu\text{g/L}$	88 $\mu\text{g/L}$
Zn^{2+}	86 $\mu\text{g/L}$	88 $\mu\text{g/L}$

process for Cu^{2+} , Zn^{2+} and ATP could be summarized in Fig. 7. **Bis-TPE** not only possessed the good sensing abilities for Cu^{2+} and Zn^{2+} , but also had the sensing abilities for ATP through double detecting processes with the “off-on” fluorescence for system of **Bis-TPE** + Cu^{2+} and “allochroic-off-on” fluorescence for system of **Bis-TPE** + Zn^{2+} + Cu^{2+} , respectively.

3.9. Application in test paper and real samples

Test strip is a convenient way to evaluate the real application prospect for sensor. Therefore, the test paper of **Bis-TPE** was prepared by immersing the neutral filter paper in a 0.1 mM solution of **Bis-TPE** for 2 min. Then the dried filter paper was obtained by volatilization at room temperature and was further customized as round slices. Three drops of a solution containing 0.1 mM of different metal ions (none, Ag^+ , Cd^{2+} , Cr^{3+} , Fe^{3+} , Hg^{2+} , K^+ , Na^+ ,

Pb^{2+} , Cu^{2+} , Sr^{2+} , Mg^{2+} , Zn^{2+} , Al^{3+} , Co^{2+} , Ni^{2+} and Ca^{2+}) were added to the test paper. Fig. 8 showed that no obvious color change was observed for the photographs of the test papers with Ag^+ , Cd^{2+} , Cr^{3+} , Fe^{3+} , Hg^{2+} , K^+ , Na^+ , Pb^{2+} , Sr^{2+} , Mg^{2+} , Al^{3+} , Co^{2+} , Ni^{2+} and Ca^{2+} . But the color of the test paper with Cu^{2+} was very faint and that with Zn^{2+} turned into yellow. These results were in accordance with the fluorescence experiment in solution and indicated the good prospect for detecting Cu^{2+} and Zn^{2+} in practical applications.

Fig. 9 exhibited the colour changes of test slices after adding sequentially Cu^{2+} -ATP and Zn^{2+} - Cu^{2+} -ATP for double detecting ATP, respectively. It can be seen that the fluorescence of **Bis-TPE** was quenched by Cu^{2+} and then the red fluorescence was recovered by the addition of ATP. On the other hand, the red fluorescence of **Bis-TPE** turned to yellow by adding Zn^{2+} . This yellow fluorescence was further quenched by adding Cu^{2+} and was lightened again by adding ATP with strong yellow fluorescence. These results

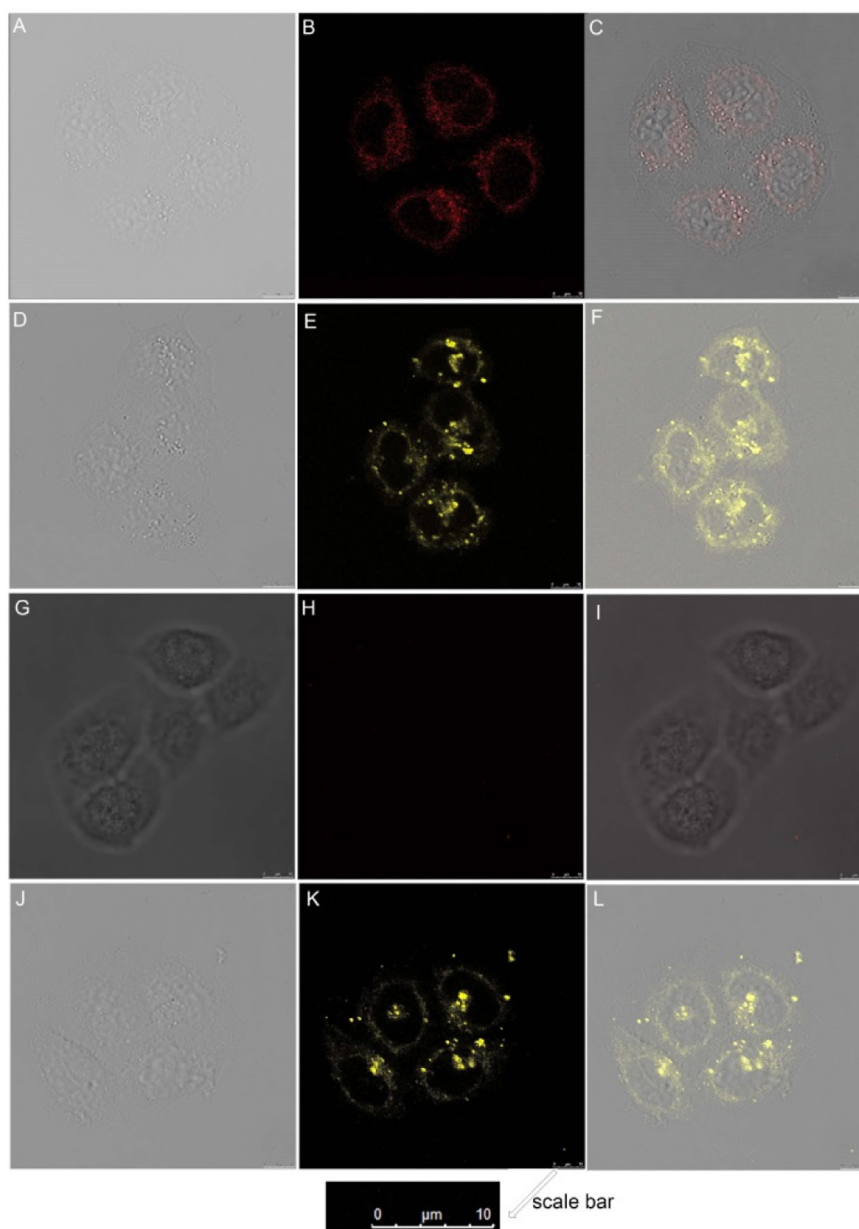


Fig. 10. Confocal fluorescence images of MCF-7 cells before and after incubated with **Bis-TPE** (1.0×10^{-5} M), metallic ions and ATP. (A)–(C) MCF-7 cells with **Bis-TPE**; (D)–(F) MCF-7 cells with **Bis-TPE** and Zn^{2+} ; (G)–(I) MCF-7 cells with **Bis-TPE**, Zn^{2+} and Cu^{2+} ; (J)–(L) MCF-7 cells with **Bis-TPE**, Zn^{2+} , Cu^{2+} and ATP. Left images were bright field images, middle images were fluorescence images, and right images were the merged images of fluorescence and bright field. ($\lambda_{\text{ex}} = 405$ nm). The same scale bar for all images (as shown for image K).

also supported that **Bis-TPE** possesses excellent off-on and allochroic-off-on fluorescence response for double detecting ATP in practical applications. On the other hand, the practical applications of detecting Cu^{2+} and Zn^{2+} were also investigated (ATP detection in practical samples was not performed because there is no ideal method available on hand for detecting ATP in controlled trials). Some Cu^{2+} and Zn^{2+} were added in real water sample of Minjiang River. Then these samples were analyzed by the fluorescence method of this work and ICP-MS, respectively. The results were summarized in Table 1. The obtained data of these two methods were almost identical with a deviation of less than 3%, suggesting again the potential of **Bis-TPE** for detecting practical samples.

3.10. Application in living cell imaging

Recently, the fluorescent probe exhibited the broad application prospects for living cell imaging. Therefore, the sensing abilities of **Bis-TPE** were used for the detecting Zn^{2+} , Cu^{2+} and ATP in living biologic cells by confocal laser scanning microscopy (CLSM). Usually, the AIE-active polymeric nanoparticles were used in biological imaging to avoiding organic solvents [62–70]. In this work, DMSO/ H_2O system was chosen as solution due to the low toxicity of DMSO and good solubility of DMSO for **Bis-TPE**. According to the published method of metabolic activity with MTT assay, **Bis-TPE** displayed low biotoxicity with above 82% of the alive MCF-7 cell at concentration of 1.0×10^{-5} M for 24 h at 37 °C (Figure S18). Then, **Bis-TPE** was tracked in MCF-7 cells by incubation for 1 h. A red fluorescence was seen in the cells (Fig. 10 B), indicating the good living cell imaging performance of **Bis-TPE**. With the addition of Zn^{2+} in **Bis-TPE**-MCF-7 system, the red fluorescence changed to bright yellow, and was then quenched by adding Cu^{2+} . After further adding ATP, the yellow fluorescence was recovered again (Fig. 10). Also, the red fluorescence in the cells with **Bis-TPE** was quenched by adding Cu^{2+} and recovered by further adding ATP (The fluorescence images were similar with Fig. 10H and B). All these experimental results suggested that **Bis-TPE** not only could sense the Cu^{2+} and Zn^{2+} in living cell system with obviously fluorescence changes, but also possessed the ability of double detecting ATP in living cells by sequentially adding Cu^{2+} -ATP with off-on red fluorescence response and sequentially adding Zn^{2+} - Cu^{2+} -ATP with allochroic-off-on red-yellow fluorescence response, respectively. This kind of double detecting ATP based on organic sensor was observed for the first time, which was obviously better than the mode of single fluorescence response and might bring the more extensive application prospects.

4. Conclusion

In summary, this paper prepared a hydrazono-bridged bis-tetraphenylethylene (**Bis-TPE**) in 82% yield with simple procedure. **Bis-TPE** exhibited good AIE fluorescence at 550–700 nm based on the large conjugated electron effect. It possessed outstanding selective sensing abilities for Cu^{2+} by strong fluorescence quenching and for Zn^{2+} by blue shift of fluorescence wavelength among 16 kinds of tested metal ions. Furthermore, the strong red fluorescence in **Bis-TPE** + Cu^{2+} system could be recovered by adding ATP. On the other hand, the orange fluorescence of **Bis-TPE** + Zn^{2+} system could be quenched by Cu^{2+} and then was recovered again by adding ATP. These results suggested that **Bis-TPE** possessed the double detecting abilities of ATP with the off-on red fluorescence for system of **Bis-TPE** + Cu^{2+} and allochroic-off-on orange fluorescence for **Bis-TPE** + Zn^{2+} + Cu^{2+} system. The 1:1 stoichiometric ratios of **Bis-TPE** with Cu^{2+} and Zn^{2+} were confirmed by ^1H NMR and MS spectra. Moreover, this sensor was also successfully used to detect Cu^{2+} , Zn^{2+} and ATP in test paper and living cell imaging, exhibiting good double detecting for ATP based on off-on and allochroic-off-

on fluorescence response.

Acknowledgment

Financial support from the National Natural Science Foundation of China (No: 21406036), Fujian Science and Technology Project (No. 2019N0010), Fuzhou science and technology project (2018-G-44), and Undergraduate innovation program of FJNU (2019) were greatly acknowledged.

Appendix A. Supplementary data

Supplementary data to this article can be found online at <https://doi.org/10.1016/j.saa.2019.117568>.

References

- [1] E.K. Feuster, T.E. Glass, Detection of amines and unprotected amino acids in aqueous conditions by formation of highly fluorescent iminium ions, *J. Am. Chem. Soc.* 125 (2003) 16174–16175.
- [2] Y. Takagai, Y. Nojiri, T. Takase, W.L. Hinze, M. Butsugan, S. Igarashi, Turn-on" fluorescent polymeric microparticle sensors for the determination of ammonia and amines in the vapor state, *Analyst* 135 (2010) 1417–1425.
- [3] A.R. Longstreet, M. Jo, R.R. Chandler, K. Hanson, N. Zhan, J.J. Hrudka, H. Mattoussi, M. Shatruk, D.T. Mcquade, Ylidenemalonitrile enamines as fluorescent "turn-on" indicators for primary amines, *J. Am. Chem. Soc.* 136 (2014) 15493–15496.
- [4] L. Dong, C. Deng, C. He, L. Shi, Y. Fu, D. Zhu, H. Cao, Q. He, J. Cheng, Highly sensitive vapor detection of amines with fluorescent conjugated polymer: a novel lasing turn-on sensory mechanism, *Sens. Actuators, B* 180 (2013) 28–34.
- [5] M. Venkateswarulu, P. Gaur, R.R. Koner, Sensitive molecular optical material for signaling primary amine vapors, *Sens. Actuators, B* 210 (2015) 144–148.
- [6] P.L. McGrier, K.M. Soltsev, S. Miao, L.M. Tolbert, O.R. Miranda, V.M. Rotello, U.H.F. Bunz, Hydroxycruciforms: amine-responsive fluorophores, *Chem. Eur J.* 14 (2018) 4503–4510.
- [7] M.T. Salazar, T.K. Smith, A. Harris, High-performance liquid chromatographic method for determination of biogenic amines in feedstuffs, complete feeds, and animal tissues, *J. Agric. Food Chem.* 48 (2000) 1708–1712.
- [8] Y. Zhang, C. Peng, X. Ma, Y. Che, J. Zhao, Fluorescent and photoconductive nanoribbons as a dual-mode sensor for selective discrimination of alkyl amines versus aromatic amines, *Chem. Commun.* 51 (2015) 15004–15007.
- [9] R. Lincoln, L.E. Greene, W. Zhang, Louisa, G. Cosa, Mitochondria alkylation and cellular trafficking mapped with a lipophilic BODIPY-acrolein fluorogenic probe, *J. Am. Chem. Soc.* 139 (2017), 16273–12261.
- [10] J. Shie, Y. Liu, Y. Lee, C. Lim, J. Fang, C. Wong, An azido-BODIPY probe for glycosylation: initiation of strong fluorescence upon triazole formation, *J. Am. Chem. Soc.* 136 (2014) 9953–9961.
- [11] G. Sivaraman, M. Iniya, T. Anand, N.G. Kotla, O. Sunnapu, S. Singaravadevi, A. Gulyani, D. Chellappa, Chemically diverse small molecule fluorescent chemosensors for copper ion, *Coord. Chem. Rev.* 357 (2018) 50–104.
- [12] J. Rosenthal, S.J. Lippard, Direct detection of nitroxyl in aqueous solution using a tripodal copper(II) BODIPY complex, *J. Am. Chem. Soc.* 132 (2010) 5536–5537.
- [13] X. Zhao, C. Ji, L. Ma, Z. Wu, W. Cheng, M. Yin, An aggregation-induced emission-based "turn-on" fluorescent probe for facile detection of gaseous formaldehyde, *ACS Sens.* 3 (2018) 2112–2117.
- [14] A. Ji, Y. Fan, W. Ren, S. Zhang, H.W. Ai, A sensitive near-infrared fluorescent sensor for mitochondrial hydrogen sulfide, *ACS Sens.* 3 (2018) 992–997.
- [15] L. Luo, Z. Xie, J.W. Lam, L. Cheng, H. Chen, C. Qiu, H.S. Kwok, X. Zhan, Y. Liu, D. Zhu, B.Z. Tang, Aggregation-induced emission of 1-methyl-1,2,3,4,5-pentaphenylsilole, *Chem. Commun.* 14 (2001) 1740–1743.
- [16] X. Yu, H. Chen, X. Shi, P. Albouy, J. Guo, J. Hu, M. Li, Liquid crystal gelators with photo-responsive and AIE properties, *Mater. Chem. Front* 2 (2018) 2245–2249.
- [17] S. Jiang, J. Qiu, Y. Chen, H. Guo, F. Yang, Luminescent columnar liquid crystals based on AIE tetraphenylethylene with hydrazone groups bearing multiple alkyl chains, *Dyes Pigm* 159 (2018) 533–541.
- [18] L. Lin, H. Guo, X. Fang, F. Yang, Novel AIE columnar liquid crystals: the influence of the number of diphenylacrylonitrile groups on the mesomorphic and fluorescence properties, *RSC Adv.* 7 (2017) 20172–20176.
- [19] H. Guo, L. Lin, J. Qiu, F. Yang, Phenylacrylonitrile-bridging triphenylene dimers: the columnar liquid crystals with high fluorescence in both solid state and solution, *RSC Adv.* 7 (2017) 53316–53319.
- [20] H. Nie, B. Chen, J. Zeng, Y. Xiong, Z. Zhao, B. Tang, Excellent n-type light emitters based on AIE-active silole derivatives for efficient simplified organic light-emitting diodes, *J. Mater. Chem. C* 6 (2018) 3690–3698.
- [21] W.W.H. Lee, Z. Zhao, Y. Cai, Z. Xu, Y. Yu, Y. Xiong, R.T.K. Kwok, Y. Chen, N.L.C. Leung, D. Ma, J.W.Y. Lam, A. Qin, B. Tang, Facile access to deep red/near-infrared emissive AIEgens for efficient non-doped OLEDs, *Chem. Sci.* 9 (2018) 6118–6125.
- [22] H. Shi, X. Zhang, C. Gui, S. Wang, L. Fang, Z. Zhao, S. Chen, B.Z. Tang, Synthesis,

- aggregation-induced emission and electroluminescence properties of three new phenylethylene derivatives comprising carbazole and (dimesitylboranyl) phenyl groups, *J. Mater. Chem. C* 5 (2017) 11741–11750.
- [23] D.D. La, S.V. Bhosale, L.A. Jones, S.V. Bhosale, Tetraphenylethylene-based AIE-active probes for sensing applications, *ACS Appl. Mater. Interf.* 10 (2018) 12189–12216.
- [24] J. Jiang, J. Qiu, L. Lin, H. Guo, F. Yang, Circularly polarized luminescence based on columnar self-assembly of tetraphenylethylene with multiple cholesterol units, *Dyes Pigm* 163 (2019) 363–370.
- [25] A. Chatterjee, M. Banerjee, D.G. Khandare, R.U. Gawas, S.C. Mascarenhas, A. Ganguly, R. Gupta, H. Joshi, Aggregation-induced emission-based chemodosimeter approach for selective sensing and imaging of Hg(II) and methylmercury species, *Anal. Chem.* 89 (2017) 12698–12704.
- [26] F. Hu, D. Mao, X. Cai, W. Wu, D. Kong, B. Liu, A light-up probe with aggregation-induced emission for real-time bio-orthogonal tumor labeling and image-guided photodynamic therapy, *Angew. Chem. Int. Ed.* 57 (2018) 10182–10184.
- [27] J. Qiu, Y. Chen, S. Jiang, H. Guo, F. Yang, A fluorescent sensor based on aggregation-induced emission: highly sensitive detection of hydrazine and its application in living cell imaging, *Analyst* 143 (2018) 4298–4305.
- [28] J. Qiu, Y. Chen, S. Jiang, H. Guo, F. Yang, An AIE and FRET-based BODIPY sensor with large Stoke shift: novel pH probe exhibiting application in CO₃²⁻ detection and living cell imaging, *Dyes Pigm* 157 (2018) 351–358.
- [29] J. Mei, Y. Huang, H. Tian, Progress and trends in AIE-based bioprobes: a brief overview, *ACS Appl. Mater. Interf.* 10 (2018) 12217–12261.
- [30] M. Kang, X. Gu, R.T.K. Kwok, C.W.T. Leung, J.W.Y. Lam, F. Li, B.Z. Tang, A near-infrared AIEgen for specific imaging of lipid droplets, *Chem. Commun.* 52 (2016) 5957–5960.
- [31] M. Donnier-Maréchal, S. Abdullayev, M. Bauduin, Y. Pascal, M. Fu, X. He, E. Gillon, A. Imbert, E. Kipnis, R. Dessein, S. Vida, Tetraphenylethylene-based glycoclusters with aggregation-induced emission (AIE) properties as high-affinity ligands of bacterial lectins, *Org. Biomol. Chem.* 16 (2018) 8804–8809.
- [32] R.T.K. Kwok, C.W.T. Leung, J.W.Y. Lam, B.Z. Tang, Biosensing by luminogens with aggregation-induced emission characteristics, *Chem. Soc. Rev.* 4 (2015) 4228–4238.
- [33] W. Wu, D. Mao, F. Hu, S. Xu, C. Chen, C.J. Zhang, X. Cheng, Y. Yuan, D. Ding, D. Kong, B. Liu, A highly efficient and photostable photosensitizer with near-infrared aggregation-induced emission for image-guided photodynamic anticancer therapy, *Adv. Mater.* 29 (2017) 1700548.
- [34] F.R. Siegel, *Environmental Geochemistry of Potentially Toxic Metals*, Springer, Berlin Heidelberg, Berlin, 2002.
- [35] P.A. Kobielska, A.J. Howarth, O.K. Farha, S. Nayak, Metal-organic frameworks for heavy metal removal from water, *Coord. Chem. Rev.* 358 (2018) 92–107.
- [36] A. Navas-Acien, E. Selvin, A.R. Sharrett, E. Calderon-Aranda, E. Silbergeld, E. Guallar, Lead, cadmium, smoking, and increased risk of peripheral arterial disease, *Circulation* 109 (2014) 3196–3201.
- [37] D. Mozaffarian, P. Shi, J.S. Morris, D. Spiegelman, P. Grandjean, D.S. Siscovick, W.C. Willett, E.B. Rimm, Mercury exposure and risk of cardiovascular disease in two U.S. cohorts, *N. Engl. J. Med.* 364 (2011) 1116–1125.
- [38] T.W. Clarkson, L. Magos, G.J. Myers, The toxicology of mercury - current exposures and clinical manifestations, *N. Engl. J. Med.* 349 (2003) 1731–1737.
- [39] B.J. Grattan, H.C. Freaque, Zinc and cancer: implications for LIV-1 in breast cancer, *Nutrients* 4 (2012) 648–675.
- [40] P. Huang, L. Feng, E.A. Oldham, M.J. Keating, W. Plunkett, Superoxide dismutase as a target for the selective killing of cancer cells, *Nature* 407 (2000) 390–395.
- [41] S.L. Sensi, P. Paoletti, A.I. Bush, I. Sekler, Zinc in the physiology and pathology of the CNS, *Nat. Rev. Neurosci.* 10 (2009) 780–791.
- [42] M.D. Pluth, E. Tomat, S.J. Lippard, Biochemistry of mobile zinc and nitric oxide revealed by fluorescent sensors, *Annu. Rev. Biochem.* 80 (2011) 333–355.
- [43] E.M. Farré, P. Geigenberger, L. Willmitzer, R.N. Trethewey, A possible role for pyrophosphate in the coordination of cytosolic and plastidial carbon metabolism within the potato tuber, *Plant Physiol.* 123 (2000) 681–688.
- [44] Y. Chen, R. Corriden, Y. Inoue, L. Yip, N. Hashiguchi, A. Zinkernagel, V. Nizet, P.A. Insel, W.G. Junger, ATP release guides neutrophil chemotaxis via P2Y2 and A3 receptors, *Science* 314 (2006) 1792–1795.
- [45] A.V. Gourine, E. Llaudet, N. Dale, K.M. Spyer, ATP is a mediator of chemosensory transduction in the central nervous system, *Nature* 436 (2005) 108–111.
- [46] S. Farshbaf, P. Anzenbacher Jr., Fluorimetric sensing of ATP in water by an imidazolium hydrazone based sensor, *Chem. Commun.* 55 (2019) 1770–1773.
- [47] X. Jin, X. Wu, B. Wang, P. Xie, Y. He, H. Zhou, B. Yan, J. Yang, W. Chen, X. Zhang, A reversible fluorescent probe for Zn²⁺ and ATP in living cells and in vivo, *Sens. Actuators, B* 261 (2018) 127–134.
- [48] Y. Liu, D. Lee, D. Wu, K.M.K. Swamy, J. Yoon, A new kind of rhodamine-based fluorescence turn-on probe for monitoring ATP in mitochondria, *Sens. Actuators, B* 265 (2018) 429–434.
- [49] L.Y. Geng, Y. Zhao, E. Kamyra, J.T. Guo, B. Sun, Y.K. Feng, M.F. Zhu, X.K. Ren, Turn-off/on fluorescent sensors for Cu²⁺ and ATP in aqueous solution based on a tetraphenylethylene derivative, *J. Mater. Chem. C* 7 (2019) 2640–2645.
- [50] A.X. Ding, Y.D. Shi, K.X. Zhang, W. Sun, Z.L. Tan, Z.L. Lu, L. He, Self-assembled aggregation-induced emission micelle (AIE micelle) as interfacial fluorescence probe for sequential recognition of Cu²⁺ and ATP in water, *Sens. Actuators, B* 255 (2018) 440–447.
- [51] L.C. Mao, Y.Z. Liu, S.J. Yang, Y.X. Li, X.Y. Zhang, Y. Wei, Recent advances and progress of fluorescent bio-/chemosensors based on aggregation-induced emission molecules, *Dyes. Pigm.* 162 (2019) 611–623.
- [52] M. Pannipara, A.G. Al-Sehemi, A. Irfan, M. Assiri, A. Kalam, Y.S. Al-Sehemi, AIE active multianalyte fluorescent probe for the detection of Cu²⁺, Ni²⁺, and Hg²⁺ ions, *Spectrochim. Acta. A* 201 (2018) 54–60.
- [53] Z.H. Xu, Y. Wang, Y. Wang, J.Y. Li, W.F. Luo, W.N. Wu, Y.C. Fan, AIE active salicylaldehyde-based hydrazone: a novel single-molecule multianalyte (Al³⁺ or Cu²⁺) sensor in different solvents, *Spectrochim. Acta. A* 212 (2019) 146–154.
- [54] H.Y. Huang, D.Z. Xu, M.Y. Liu, R.M. Jiang, L.C. Mao, Q. Huang, Q. Wan, Y.Q. Wen, X.Y. Zhang, Y. Wei, Direct encapsulation of AIE-active dye with β -cyclodextrin terminated polymers: self-assembly and biological imaging, *Mat. Sci. Eng. C-Mater.* 78 (2017) 862–867.
- [55] J.W. Tian, R.M. Jiang, P. Gao, D.Z. Xu, L.C. Mao, G.J. Zeng, M.Y. Liu, F.J. Deng, X.Y. Zhang, Y. Wei, Synthesis and cell imaging applications of amphiphilic AIE-active poly(amino acid)s, *Mat. Sci. Eng. C-Mater.* 79 (2017) 563–569.
- [56] L. Lan, Q. Niu, Z. Guo, H. Liu, T. Li, Highly sensitive and fast responsive “turn-on” fluorescent sensor for selectively sensing Fe³⁺ and Hg²⁺ in aqueous media based on an oligothiophene derivative and its application in real water samples, *Sens. Actuators, B* 244 (2017) 500–508.
- [57] Y. Li, Y. Liu, H. Zhou, W. Chen, J. Mei, J. Su, Ratiometric Hg²⁺/Ag⁺ Probes with orange red-white-blue fluorescence response constructed by integrating vibration-induced emission with an aggregation-induced emission motif, *Chem. Eur. J.* 23 (2017), 9280–9287.
- [58] J.L. Vinkenborg, S.M.J. Van, Duijnhoven, M. Merckx, Reengineering of a fluorescent zinc sensor protein yields the first genetically encoded cadmium probe, *Chem. Commun.* 47 (2011) 11879–11881.
- [59] W.Z. Yuan, Z.Q. Yu, P. Lu, C. Deng, J.W.Y. Lam, Z. Wang, E.Q. Chen, Y. Ma, B.Z. Tang, High efficiency luminescent liquid crystal: aggregation-induced emission strategy and biaxially oriented mesomorphic structure, *J. Mater. Chem.* 22 (2012) 3323–3326.
- [60] Q. Niu, T. Sun, T. Li, Z. Guo, H. Pang, Highly sensitive and selective colorimetric/fluorescent probe with aggregation induced emission characteristics for multiple targets of copper, zinc and cyanide ions sensing and its practical application in water and food samples, *Sens. Actuators, B* 266 (2018) 730–743.
- [61] S. Goswami, S. Paul, A. Manna, A differentially selective chemosensor for aratiometric response to Zn²⁺ and Al³⁺ in aqueous media with applications for molecular switches, *RSC Adv.* 3 (2013) 25079–25085.
- [62] X.Y. Zhang, K. Wang, M.Y. Liu, X.Y. Zhang, L. Tao, Y.W. Chen, Y. Wei, Polymeric AIE-based nanopores for biomedical applications: recent advances and perspectives, *Nanoscale* 27 (2015) 11486–11508.
- [63] Q. Wan, Q. Huang, M.Y. Liu, D.Z. Xu, H.Y. Huang, X.Y. Zhang, Y. Wei, Aggregation-induced emission active luminescent polymeric nanoparticles: non-covalent fabrication methodologies and biomedical applications, *Appl. Mater. Today* 06 (2017) 145–160.
- [64] Z. Long, M.Y. Liu, R.M. Jiang, Q. Wan, L.C. Mao, Y.Q. Wan, F.J. Deng, X.Y. Zhang, Y. Wei, Preparation of water soluble and biocompatible AIE-active fluorescent organic nanoparticles via multicomponent reaction and their biological imaging capability, *Chem. Eng. J.* 308 (2017) 527–534.
- [65] Z. Long, M.Y. Liu, Q. Wan, L.C. Mao, H.Y. Huang, G.J. Zeng, Y.Q. Wan, F.J. Deng, X.Y. Zhang, Y. Wei, Ultrafast preparation of AIE-active fluorescent organic nanoparticles via a “one-pot” microwave-assisted Kabachnik–Fields reaction, *Polym. Chem-UK* 37 (2016) 5644–5654.
- [66] Z. Long, M. Liu, K. Wang, F.J. Deng, D.H. Xu, L.J. Liu, Y.Q. Wan, X.Y. Zhang, Y. Wei, Facile synthesis of AIE-active amphiphilic polymers: self-assembly and biological imaging applications, *Mat. Sci. Eng. C-Mater.* 66 (2016) 215–220.
- [67] L. Huang, S.J. Yang, J.Y. Chen, J.W. Tian, Q. Huang, H.Y. Huang, Y.Q. Wen, F.J. Deng, X.Y. Zhang, Y. Wei, A facile surface modification strategy for fabrication of fluorescent silica nanoparticles with the aggregation-induced emission dye through surface-initiated cationic ring opening polymerization, *Mat. Sci. Eng. C-Mater.* 94 (2018) 270–278.
- [68] R. Jiang, M.Y. Liu, H.Y. Huang, L.C. Mao, Q. Huang, Y.Q. Wen, Q.Y. Cao, J.W. Tian, X.Y. Zhang, Y. Wei, Facile fabrication of organic dyed polymer nanoparticles with aggregation-induced emission using an ultrasound-assisted multicomponent reaction and their biological imaging, *J. Colloid Interface Sci.* 519 (2018) 137–144.
- [69] H. Huang, M.Y. Liu, R.M. Jiang, J.Y. Chen, L.C. Mao, Y.Q. Wen, J.W. Tian, N.G. Zhou, X. Y. Zhang, Y. Wei, Facile modification of nanodiamonds with hyperbranched polymers based on supramolecular chemistry and their potential for drug delivery, *J. Colloid Interface Sci.* 513 (2017) 198–204.
- [70] X.Y. Zhang, X.Q. Zhang, B. Yang, W.Y. Liu, Y.W. Chen, Y. Wei, Fabrication of aggregation induced emission dye-based fluorescent organic nanoparticles via emulsion polymerization and their cell imaging applications, *Polym. Chem-UK* 5 (2013) 399–404.